V－5

Shear Resisting Behavior of Bridge Pier Retrofitted with Carbon Fiber Sheet

Gabriel Sîrbu, Hokkaido University, Division of Structural and Geotechnical Engineering
Kimura Tsutomu, Hokkaido University, Division of Structural and Geotechnical Engineering
Yasuhiko Sato, Hokkaido University, Division of Structural and Geotechnical Engineering
Tamon Ueda, Hokkaido University, Division of Structural and Geotechnical Engineering

1. INTRODUCTION

In order to improve the performance of reinforced concrete (RC) bridge piers and RC columns subjected to seismic actions, one possibility is to apply a retrofitting method with one of the different types of plastic reinforcements available in the market. In this study, the retrofitting material is an unidirectional carbon fiber sheet (CFS) impregnated with epoxy resin. The target of this study is to determine the influence of cyclic loading and amount of CFS on the shear capacity of RC bridge piers.

2. EXPERIMENTS

2.1. Test specimens

Each specimen tested was a single prismatic column with a rigid footing. The cross-section of the column was rectangular (25×25cm) with rounded corners (R = 3.5cm). The column length was 100cm. All specimens were designed according to "Standard Specifications for Design and Constructions for Concrete Structures - 1986(Part 1 - Design)"[1]. For determining the shear capacity of each specimen a static loading test and three cyclic tests were carried out. Strains in longitudinal and transverse reinforcements and CFS, and lateral deflections were measured during each test.

2.2. Material characteristics

For each specimen, concrete compressive strength and reinforcement mechanical properties were measured. The steel reinforcement was 5 D25 (SR30) for longitudinal reinforcement (symmetric reinforcement), and round bar ø6 for transverse reinforcement at 15cm spacing. The resulting reinforcement ratio was 4.68% and 0.15% for longitudinal and for transverse reinforcement respectively.

Table 1 Mechanical properties of reinforcement

Material	Type	Cross-sectional area (cm^2)	Young's modulus (GPa)	Yield strength (MPa)	Tensile strength (MPa)
Steel	Ø6	0.28	196	226	343
	D25	5.067	188	382	-
CFS	FTS-C1-20	0.111 for 10cm width	230	-	3480

Table 2 Details of the specimens

Specimens	f'c (MPa)	Concrete Young's Modulus (GPa)	Concrete Shear Modulus (GPa)	CFS	Peak value of shear force (kN)	Test type
S1	25.7	19.0	11.60	No	143.1	Monotonic
S2	28.4	20.8	12.90	No	142.6	Cyclic
S3	22.7	19.6	9.80	5 stripes of 2cm width at 9.5cm spacing	163.2	Monotonic
S4	29.0	21.7	10.90	5 stripes of 2cm width at 9.5cm spacing	125.4	Cyclic
S5	29.3	21.0	10.50	9 stripes of 2cm width at 4.75cm spacing	203.7	Cyclic

The stress-strain relationship for the longitudinal reinforcement is a bilinear relation and for the transverse reinforcement is linear elastic until yielding and after yielding it goes directly to a strain-hardening slope up to a stress of 343MPa (3500kgf/cm²). The CFS was made by TONEN Corporation. The stress-strain relationship of CFS is linear elastic until failure. The mechanical properties of the reinforcement are presented in Table 1. The compressive strength of concrete is presented in Table 2.

2.3. Test setup and instrumentation

All specimens were tested on a rigid steel reaction frame. The reaction frame was connected to the floor (50cm thickness) with 6 Ø22 mm high-strength steel rods, and the specimen itself was connected to the reaction wall with 4 Ø32 mm high-strength steel rods. An ±294 kN (±15cm maximum displacement range) actuator was used to apply the lateral load. Figure 1 shows the test setup.

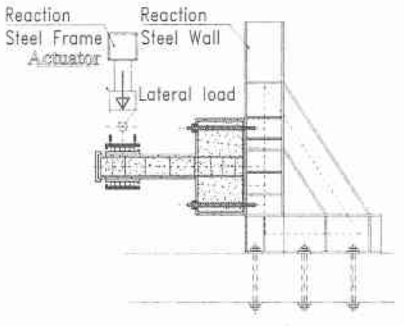

Figure 1 Test setup

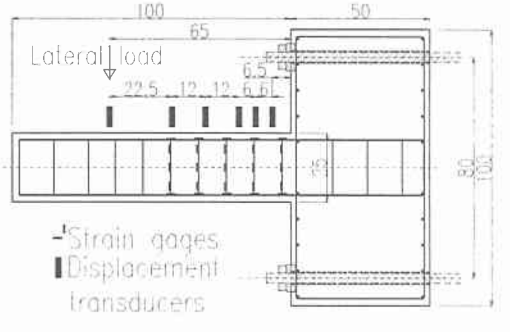

Figure 2 Strain gages and transducers arrangement

Figure 2 indicates the steel reinforcement strain gages and displacement transducers location for all specimens. Each stirrup had 6 strain gages; for the longitudinal bars, the middle one had 4 strain gages at 15cm spacing, starting from the base. Figure 3 shows the position of CFS strain gages for specimens S3 and S4. Figure 4 shows the position of CFS strain gages for specimen S5. After each step in the loading history, all data were scanned and recorded.

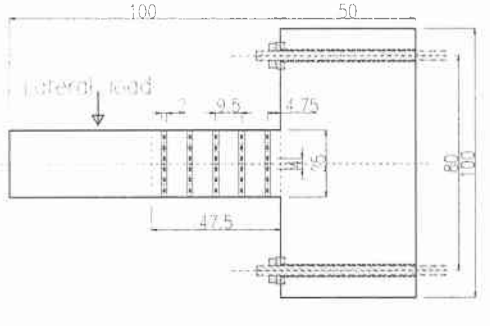

Figure 3 CFS strain gages in specimens S3 and S4

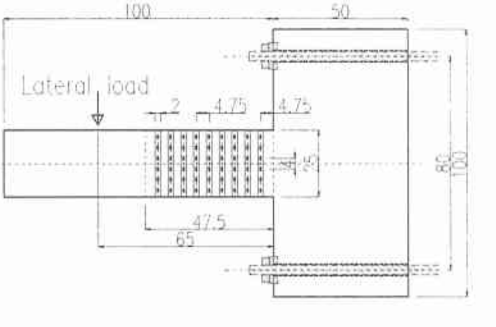

Figure 4 CFS strain gages in specimen S5

3. TEST RESULTS

3.1. Test observations

For specimen S1 after the first shear crack formed, with the increase of the lateral load additional shear cracks formed. These cracks extended and became a major shear crack that can be represented by a line which links the loading point with the opposite point at the base of the column. Specimen S2 had a similar behavior and a symmetric crack pattern formed.

For specimen S3 after a shear crack formed, delamination of CFS stripes in the vicinity of the shear crack occurred with the increase of the load until the failure. The delamination could be observed in the epoxy resin layer which presented very fine cracks near the CFS stripes. The specimen S4 had a different behavior and did not present very clear delamination phenomena. Due to this fact very localized stress could develop in the CFS stripes. As a result, they broke almost along the same line that the shear cracks intersected them. Same symmetric crack pattern was observed.

For specimen S5 the same symmetric crack pattern was observed but in this case the delamination occurred clearly. The CFS stripes that failed first were in the region where the two symmetric main shear cracks intersected. Also the delamination phenomena observed in this case occurred with a lower speed compared with the case of specimen S3.

The peak value for the shear resisting force for specimen S1 was 143.1kN. For specimen S2 the peak value was 142.6kN. Specimen S3, which had 5 stripes of CFS had the peak value of 163.2kN. This increase in the peak value is due to the CFS retrofitting. For specimen S5 the peak value increased up to 203.7kN. This increase was due to the bigger CFS reinforcing ratio.

Specimen S4 had the lowest peak value. After the CFS stripes broke, the peak value was 125.4kN. Until now we cannot explain why this value was less than the peak value of specimen S1 or S2.

3.2. Displacement versus lateral load

Specimens S1 and S3 were statically and monotonically loaded until failure. The yielding of longitudinal bars for specimen S1 occurred at the lateral displacement of 11mm. Specimens S2, S4 and S5 were subjected to the loading history presented in Figure 5. For this loading history, $0.2\delta_y$ of S1 was chosen as step for each 4 cycles series.

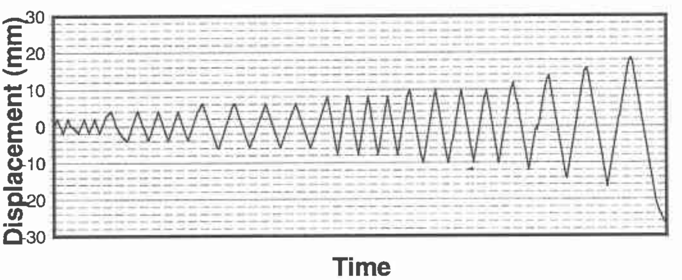

Figure 5 Loading history

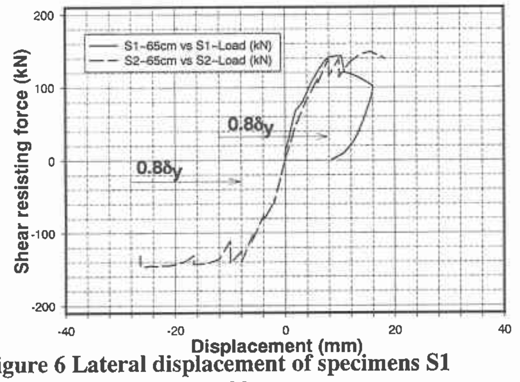

Figure 6 Lateral displacement of specimens S1 and S2

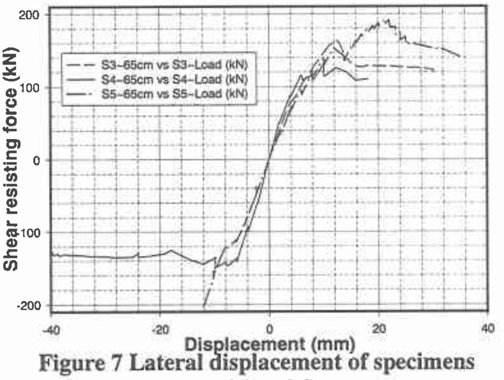

Figure 7 Lateral displacement of specimens S3, S4 and S5

Figure 6 presents the plot of displacement versus shear resisting force for specimen S1 and the envelope of specimen S2. Specimen S2 starts to present visible degradation of the shear resisting force within the same series of cycles from the series of $0.8\delta_y$. Even with this degradation, the specimen S2 can be characterized with an envelope curve which fits the displacement versus shear resisting force curve of specimen S1.

Figure 7 presents the plot of displacement versus shear resisting force for specimen S3 and envelope of specimen S4 and S5. Specimen S3 reached the maximum shear resisting force of 163.2kN at 12.63mm lateral displacement. After that moment the CFS stripes broke one after an other. In specimen S4 CFS stripes failed suddenly at the beginning of $0.8\delta_y$ series. The peak value on the plot was the last recorded value prior to the breakage of CFS stripes. The failure of the CFS stripes was due to the localized stress concentration at the location of the shear crack. Specimen S5 reached the maximum shear resisting force of 203.7kN at –12.06mm lateral displacement and then, specimen S5 showed a degradation in the shear resisting force in the other direction. After increasing further the displacement in this direction the shear resisting force started to increase again until the ultimate value of 191.3kN at 22.05mm lateral displacement.

3.3. Strains versus lateral load

Figure 8 presents the maximum strain recorded in the stirrups (on the left side of the specimen; the right side is similar) for all specimens.

Figure 9 presents the maximum strain recorded in the CFS stripes.

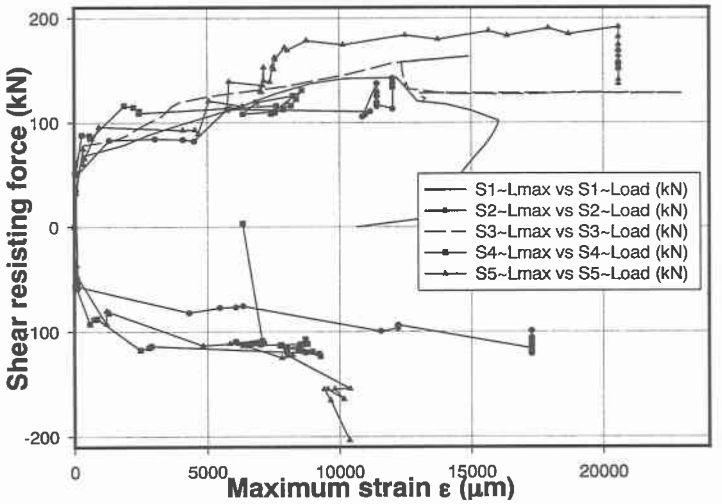

Figure 8 Maximum strain in stirrups

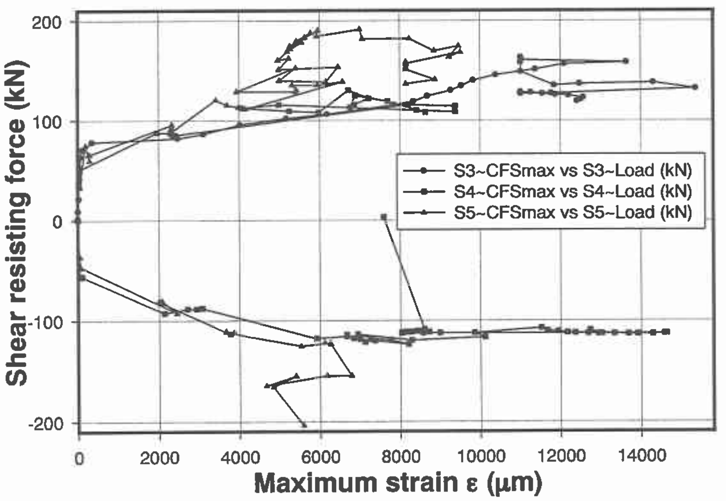

Figure 9 Maximum strain in CFS

For specimen S2, after the first shear crack formed, it was observed that the maximum strain value recorded in the stirrups within the same cycle series did not change significantly, which means that the shear force carried by stirrups does not change significantly. However, the shear resisting force decrease during the four cycles of each loading step. This leads to the conclusion that the reduction of the resisting shear force for the same displacement is caused mainly by the reduction of the shear force carried by the concrete. The peak value for the shear resisting force is under the curve plotted for specimen S1.

For specimen S3, the component of the shear resisting force carried by the stirrups increased continuously until the peak value of the shear resisting force was reached.

For specimens S4 and S5 with CFS it was observed also that during the same series of loading cycles the strain in the stirrups did not change significantly, having a similar behavior as specimen S2 without CFS.

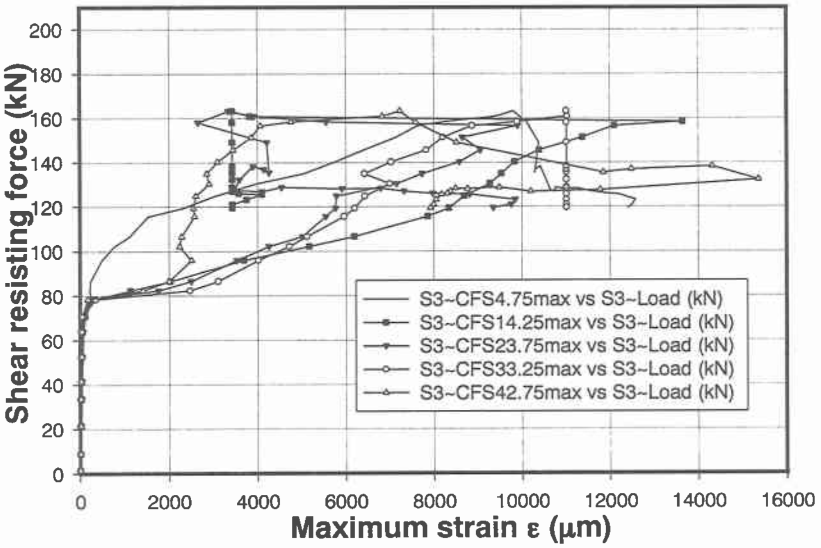

Figure 10 Maximum strain in CFS of specimen S3

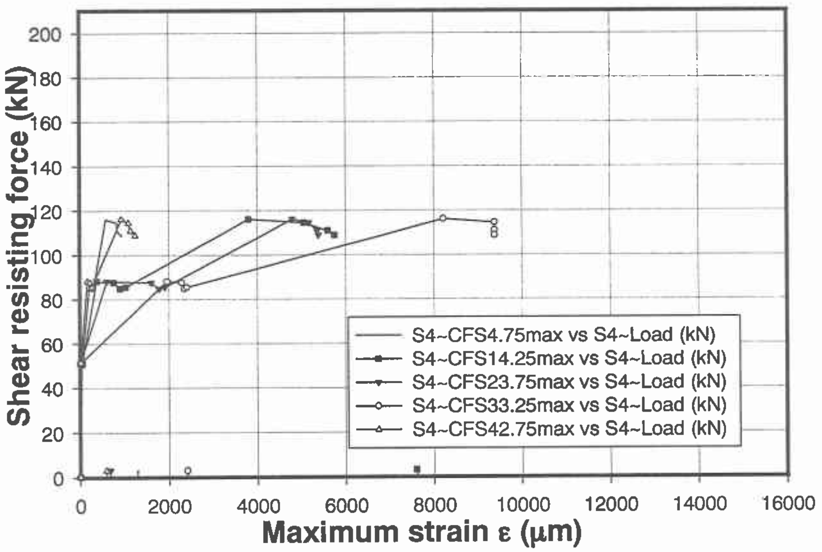

Figure 11 Maximum strain in CFS of specimen S4

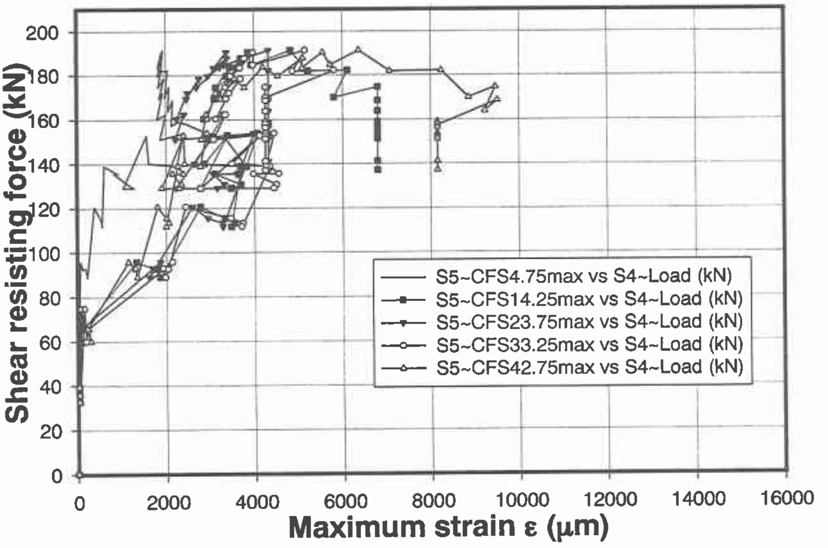

Figure 12 Maximum strain in CFS of specimen S5

Figure 10, Figure 11 and Figure 12 present plots at the same scale of the maximum values of the strains recorded in CFS stripes for specimens S3, S4 and S5 respectively (for S5 only the corresponding stripes from S3 and S4 were plotted). Specimen S5 had CFS reinforcement ratio almost double of the CFS reinforcing ratio for specimens S3 and S4. After the shear crack occurred, the recorded values of the strains in CFS stripes at the same location for specimen S5 are about one half of the recorded values of the strains in CFS stripes at the same location for specimen S3 and specimen S4.

4. CONCLUSIONS

- The degradation of shear resisting force under cyclic loading within $1\delta_y$ for the retrofitted specimens was caused mainly by the reduction of the resisting shear force component carried by concrete, which triggers the degradation of the component carried by the stirrups.
- After the shear crack occurs, the envelope values of the shear resisting force carried by CFS stripes are linearly dependent on the CFS reinforcing ratio.

REFERENCES

[1] JSCE, "Standard Specifications for Design and Construction for Concrete Structures - 1986(Part 1-Design)".